

Influence of the longitudinal magnetic field on the turning angle of a cylindrical bar-shaped magnetorheological elastomer

I. BICA^a, M. BALASOIU^{b,c*}, M. BUNOIU^a, L. IORDACONU^a, G. CIRTINA^a

^aUniversity of Timișoara, Faculty of Physics, 300223 Timișoara, România

^b"Horia Hulubei" National Institute of Physics and Engineering, P.O.Box.MG-6, Bucharest, Romania

^cJoint Institute for Nuclear Research, 141980, Dubna, Russian Federation

A magnetorheological elastomer (MRE) is fabricated, with Fe microparticles in the shape of chains, parallel among themselves and parallel with the cylindrical bar generator ($\varnothing 36 \times 62 \text{ mm}^2$). For constant values of the moment of force Γ , we measure the rotation angle of the cylindrical bar in longitudinal magnetic field with intensities in the range $0 \leq H(\text{kA/m}) \leq 200$. For the cylindrical bar with undefined flat sections, the turning angle is also determined as a function of H , for constant values of Γ . It is shown that the rigidity of MRE is increased under the influence of the longitudinal magnetic field. The obtained results are presented and discussed.

(Received August 13, 2015; accepted September 9, 2015)

Keywords: magnetorheological elastomer, longitudinal magnetic field, turning angle, iron microparticles, silicone rubber.

1. Introduction

Magnetorheological and magnetic elastomers (MREs and MEs) are made of elastic matrices in which magnetizable micro- and nanoparticles have stable positions in time [1-3]. Magnetorheological suspensions (MRS) [4-6] and elastomers (MREs)[1-3, 7-17] have physical characteristics that are dependent on the properties and on the volume concentration of the magnetizable phase [10, 11, 15]. As active magnetically material, MREs are used in achieving passive and active elements of electric circuits [9-14,18,19] and in equipping vibration and mechanical shocks mufflers [20-23]. Active research for the fabrication of new MREs [18, 19] and MEs, experimental, theoretical and computer simulation investigation of their structural [24-31] and macroscopic properties are in progress.

Production of magneto-mechanical devices for operation in unfriendly environments is of great interest nowadays, and for this purpose MREs is a promising active magnetic material [13]. Thus, the knowledge of the response function of MREs under external magneto-mechanical actions is very important. In this paper, we address this issue and the turning angle of cylindrical bar-shaped MREs is determined, as a function of magnetic field intensity at fixed values of the moment of force (torque).

2. Experimental

2.1 Materials

The materials used for the production of MRE are:

- silicone rubber (SR), type RTV 3325, from Bluestar - Silicones;
- catalyst (C), type 60R from Rhone - Poulenc,
- magnetorheological suspension (MRS) based on silicone oil (SO) and carbonyl iron (CI).

2.2 Methods

The materials CI and SO are of Merck type. CI is a powder with granulation ranging between $4.5 \mu\text{m}$ and $5.4 \mu\text{m}$. The iron content of CI is min. 97%. MRS is obtained by using the procedure described in Ref. [18]. The mixture formed of $8 \cdot 10^{-6} \text{ m}^3$ CI and $8 \cdot 10^{-6} \text{ m}^3$ SO is kept at $T = 580\text{K} \pm 10\%$, for ~ 600 s. During this time, CI decomposes into iron atoms and carbon oxides. The Fe atoms condense in nucleation points of the solution [18]. Fe particles (IM's) formed in SO have the shapes and sizes shown in Fig. 1a. The particle size distribution is shown in Fig. 1b as relative frequency f_r function of the diameter d . The mean diameter of the IM's is $d_m = 0.435 \mu\text{m}$. The IMs together with SO compose what is known as MRS [9-11, 18].

A volume of MRS, at $T \approx 300$ K is properly mixed with $35 \cdot 10^{-6} \text{ m}^3$ SR. Further, $35 \cdot 10^{-6} \text{ m}^3$ of C is introduced in the mixture. The mixture is homogenized, and introduced into a non-magnetic cylinder. The length of the cylinder is of 0.062 m and its inner diameter is 0.036 m.

The cylinder filled with the solution made up of SR (67% vol.), SO (8% vol.), IM`s (15% vol.) and C (10% vol.) is placed between the poles of a Weiss electromagnet. Along the cylinder, the field is set at $H_{\text{max}} = 400 \text{ kA/m}$. After about 4 hours, the SR has polymerized. The final product obtained has a cylindrical bar ($\varnothing 36 \times 62 \text{ mm}^2$) shape.

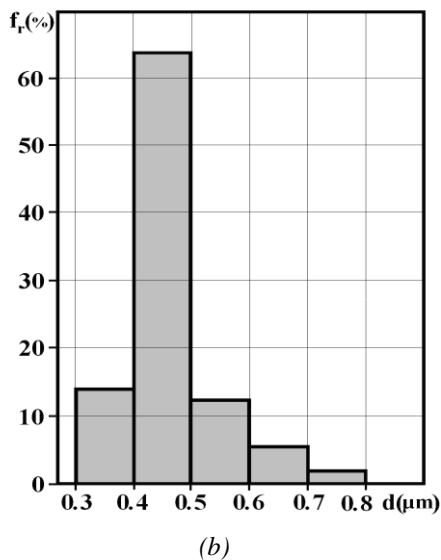
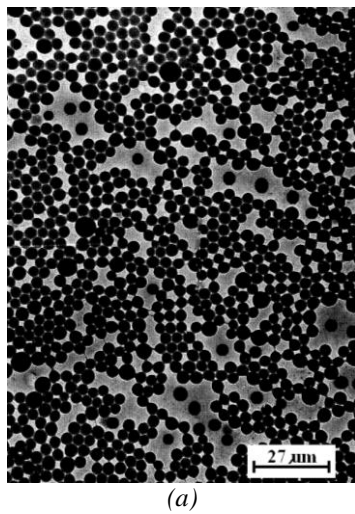


Fig.1. IM`s: a) shapes and sizes from EM image; b) size distribution: relative frequency f_r function of the diameter d .

Longitudinal cross sections of the cylindrical bar are studied by transmission X-ray microscopy method (TXM). It can be observed that chains of IM`s are formed. The chains are parallel among themselves and with the TXM image of the cylinder (Figure 2a). Also, it can be observed that IM`s are finely dispersed in the elastic matrix (Figure 2b). The magnetization curve of MRE is obtained using

the “conventional AC method” [19] and has the shape shown in Fig. 3.

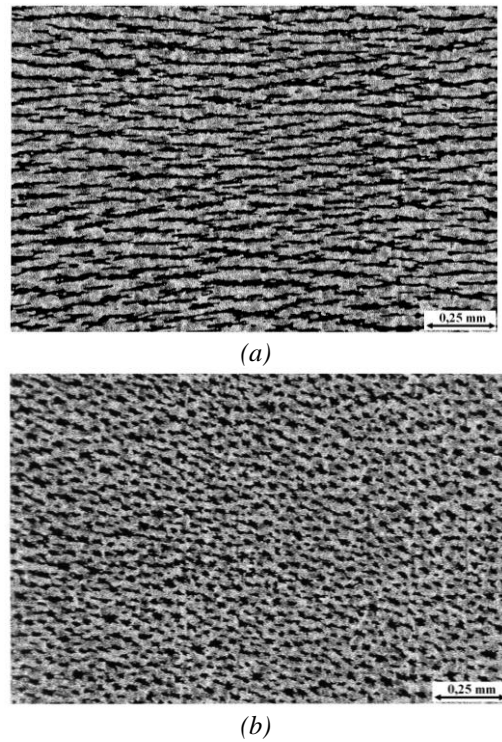


Fig.2. IM`s in SR by means TXM: a) longitudinal section; b) cross section.

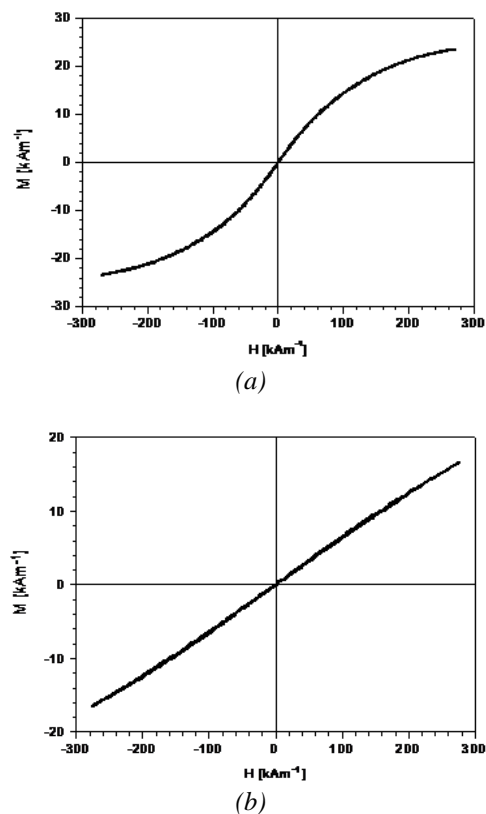


Fig. 3. Magnetization function of the MRE (M versus the intensity H of the magnetic field): a) longitudinal section; b) cross section.

3. Experimental device

The experimental device (Fig. 4) includes the electromagnet A, the steady current source B and the Gauss-meter C with a Hall probe. The cylinder bar is placed between the poles N and S. The bases of the bar are fixed rigidly, one upon N and the opposite one upon an aluminum disk. Between the disk and the S pole of A, a distance of $0.0035\text{ m} \pm 0.0005\text{ m}$ is set.

An indicator handle is fixed on the disk. The tip of the indicator handle is pointed to a millimeter graded dial. A rotation of the disk of 0.0057 rad corresponds to a movement of the indicator handle along the dial of 0.001 m . The moment of force $\vec{\Gamma}$ is applied to the diameter of the aluminum disk

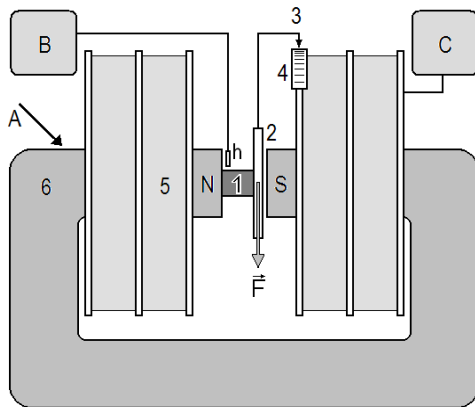


Fig.4. Experimental device (overall layout): A, Weiss electromagnet (type Phylotex-Germany); B, Gauss-meter (type GM-04) with a Hall probe h; C, current source (type CAB EC 3010); N and S, polar parts; \vec{F} , force; 1, cylindrical bar; 2, aluminum disk ($\varnothing 120 \times 0.5\text{ mm}^2$); 3, indicator handle (length 0.175 m); 4, dial; 5, coil; 6, magnetic core.

4. Results and discussions

The experimental device used for the study of the influence of the intensity of the longitudinal magnetic field upon the turning angle of MRE, in the shape of cylindrical bar, is shown in Figure 4. The torque $\vec{\Gamma}$ is applied in such way that the cylindrical bar not makes an arrow. For $\vec{\Gamma} = 0$ and $H \geq 100\text{ kA/m}$, the cylindrical bar shows no deformation of volume and, respectively, it shows no deformation of shape. $\vec{\Gamma}$ is fixed and the rotation angle of the cylindrical bar is measured, in absence of a magnetic field. The values found are those given in Fig 5.

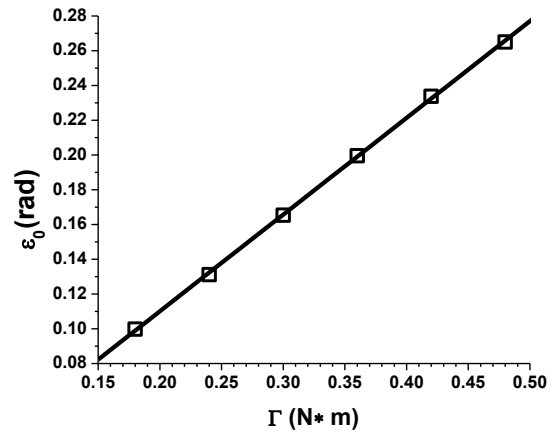


Fig.5. The rotation angle ε_0 of the cylindrical bar, based on MRE, function of the torque $\vec{\Gamma}$ for $H = 0$.

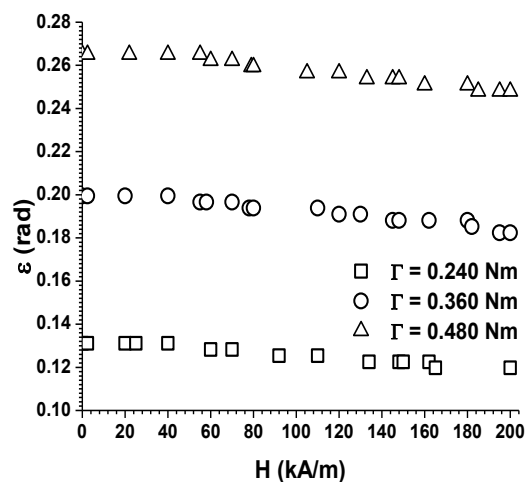


Fig.6. The turning angle ε function of H , for various values of $\vec{\Gamma}$ as parameter.

It can be observed in Fig. 5 that the angular deformations of cylindrically shaped MRE bar, increase linearly with the increase of $\vec{\Gamma}$ (i.e. with the increase of the shearing stress). The magnetic field \vec{H} is applied parallel to the symmetry axis of the cylindrical bar. $\vec{\Gamma}$ is set fixed, and for each value of \vec{H} the rotation angle of MRE in the shape of cylindrical bar is read. The obtained values are presented in Fig. 6.

It can be observed in Fig. 6 that ε decreases with the increase of H , for fixed values of $\vec{\Gamma}$. The plane-parallel bases are parallel for $0.240 \leq \Gamma$ (Nm) ≤ 0.480 . Also, the two plane-parallel sections in the cylindrical bar stay plane-parallel after turning. The lower base ($x_3 = 0$) of the bar is fixed (Fig. 7). Then, it is natural to assume that the turning angle is proportional with the length h of the cylindrical bar [33]:

$$\varepsilon = \alpha \cdot h \tag{1}$$

in which α is the rotation angle per unit length of the cylindrical bar. The relation (1) is valid for a MRE in the shape of cylindrical bar, in absence and respectively in the presence of longitudinal magnetic field.

In Fig. 6, ε is so selected that $\varepsilon_1(H) \neq \varepsilon_2(H)$. The values thus selected are introduced in (1) and for $h = 0.062\text{m}$, one obtains: $\alpha = \alpha(H)_r$, and $\alpha_0 = \alpha(0)_r$.

It is calculated the ratio $\left(\frac{\alpha_0}{\alpha(H)}\right)_r$ and obtained the graphs in Fig. 8.

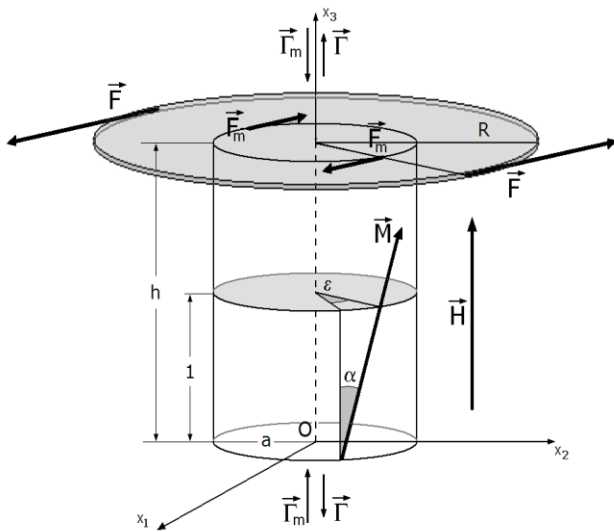


Fig.7. The cylindrical bar with undeformed flat sections: $OX_1X_2X_3$, coordinate system; \vec{F} , force; $\vec{\Gamma}$, torque; $\vec{\Gamma}_m$, magnetic moment torque; $2R$, disk diameter; “ a ”, MRE in the shape of cylindrical bar radius; \vec{H} , magnetic field intensity; \vec{M} , magnetization; α , turning angle; ε , rotation angle.

It can be observed in Fig. 8 that, for fixed Γ , the turning angle increases with H . For $H = 200 \text{ kA/m}$, the increase of α is of 10%, as compared with the value of the turning angle of MRE in the shape of cylindrical bar, in absence of a longitudinal magnetic field and with $\vec{\Gamma}$ fixed.

The IM`s in the matrix considered to be perfectly elastic become magnetized in the presence of \vec{H} . In the dipolar approximation [21], the magnetic moment of a chain can be considered identically equal to that of a magnetic dipole that is:

$$m = \frac{\pi}{6} d_m^3 \chi_p \vec{H} \tag{2}$$

in which $d_m = 0.435 \mu\text{m}$ is the diameter of the IM`s. The magnetic susceptibility of IM`s is $\chi_p = 3\beta$, where $\beta = (\mu_p - \mu_e) / (\mu_p + 2\mu_e)$ is the contrast factor [21]. In this expression, μ_p and μ_e are the relative magnetic permeabilities of IM`s and respectively of the perfect elastic matrix, respectively. Because $\mu_p \gg \mu_e = 1$, it results that $\beta = 1$ and $\chi_p = 3$, the expression (2) therefore becoming:

$$\vec{m} = 0.5\pi d_m^3 \vec{H} \tag{2'}$$

If $V = \pi a^2 h$ is the volume of the MRE, $V_e = 0.25\pi d_m^2 h$ is the volume of a chain formed of IM`s, and Φ is the volume fraction of the magnetic phase, then the number of chains formed in the elastic matrix can be calculated with the formula:

$$N_e = \frac{\Phi \cdot V}{V_e} = 4\Phi \left(\frac{a}{d_m}\right)^2, \tag{3}$$

in which the notations used are the known ones.

In the presence of a magnetic field, the MRE in the shape of cylindrical bar (Figure 7) has the magnetic moment $\vec{M} = N_e \cdot \vec{m}$ which, with (2') and (3), becomes:

$$\vec{M} = 2\pi a^2 d_m \Phi \vec{H} \tag{4}$$

The direction of \vec{M} is that of the N_e chains with magnetic dipoles. By turning, \vec{M} forms angles α with the direction of \vec{H} , as shown in Fig. 7.

The dipoles columns N_e , are considered as a permanent magnet whose magnetization equals that of MRE. In magnetic field, it takes place a rotation movement of the magnet, where the rotational moment is

$$\vec{\Gamma}_m = \mu_0 \vec{H} \times \vec{M} \tag{5}$$

in which $\mu_0 = 4\pi \cdot 10^{-7} \text{ H/m}$ is the magnetic permeability of the vacuum. $\vec{\Gamma}_m$ has the direction and sense contrary to those of $\vec{\Gamma}$. Therefore, in the presence of \vec{H} , we obtain that $\alpha < \alpha_0$, for fixed $\vec{\Gamma}$.

At equilibrium, the following equality holds

$$|\vec{\Gamma}| = |\vec{\Gamma}_m| \text{ or } \frac{2RF}{h}(d_0 - d) = \mu_0 NM\alpha, \quad (5')$$

in which case:

$$\frac{\alpha_0}{\alpha} = 1 + \frac{\mu_0 HMh}{2RF}. \quad (6)$$

Accordingly, using Eq. (4) we have

$$\frac{\alpha_0}{\alpha} = 1 + 2\pi\mu_0 a^2 d_m \frac{H^2}{\Gamma}, \quad (7)$$

in which the notations used are the known ones.

However, the proposed model does not consider the internal magnetic field; the existence of chain fragments with magnetic dipoles, due to the turning of MRE; the internal friction; also, it does not consider the magnetic interactions between the magnetic dipole chains. Therefore, Eq. (7) does not verify satisfactorily the experimental data.

This implies a more general model is needed, and by changing Eq. (7) according to:

$$\frac{\alpha_0}{\alpha} = 1 + 2\pi\mu_0 a^2 d_m \Omega \frac{H^n}{\Gamma}, \quad (8)$$

a better agreement can be obtained. Here Ω and n have a dimensionless values.

Considering the experimental data in Figure 8 and respectively, for $\mu_0 = 12.56 \cdot 10^{-7}$ H/m; $a = 0.018$ m; $d_m = 0.435\mu\text{m}$ and values of Γ , one obtains:

$$\begin{aligned} n = 1.4 \text{ and } \Omega = 7.90, & \text{ at } \Gamma = 0.240 \text{ N}\cdot\text{m}; \\ n = 1.4 \text{ and } \Omega = 6.32, & \text{ at } \Gamma = 0.360 \text{ N}\cdot\text{m}; \\ n = 1.4 \text{ and } \Omega = 6.20, & \text{ at } \Gamma = 0.480 \text{ N}\cdot\text{m}. \end{aligned} \quad (9)$$

We introduce the values for n and Ω from (9) into (8) and obtain α_0/α function of H . It can be observed from Fig. 8 that the agreement between the theoretical values and experimental data is much better.

It is well known that the total torque moment acting on the stub is [34]:

$$\Gamma_0 = RF\alpha_0 h = 0.5\pi G_0 a^2 / h, \text{ for } H = 0$$

or

$$\Gamma = RF\alpha h = 0.5\pi G a^2 / h, \text{ for } H \neq 0.$$

where G_0 and G stand for the Poisson modulus for $H = 0$ and $H \neq 0$, respectively. This leads to

$$\frac{\alpha_0}{\alpha} = \frac{G_0}{G} \quad (10)$$

which also means that the quotient $\frac{G_0}{G} = \frac{G_0}{G}(H)_\Gamma$ is identical with the one from Figure 8, with

$\frac{\alpha_0}{\alpha} = \frac{\alpha_0}{\alpha}(H)_\Gamma$. This means that under the influence of the longitudinal magnetic field the MRE-rigidity increases.

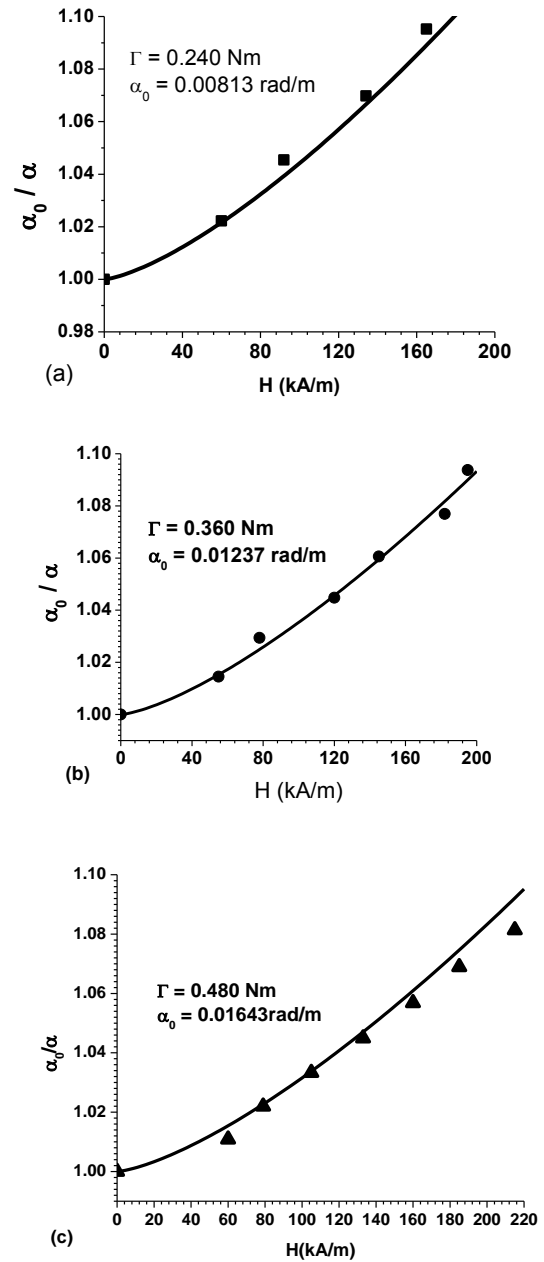


Fig. 8. α_0/α function of H , for: a) $\Gamma = 0.240$ N·m; b) $\Gamma = 0.360$ N·m; c) $\Gamma = 0.480$ N·m; ■, ●, ▲ experimental data; — theoretical values calculated with the formula (8); Note: α_0 is the turning angle of MRE in the shape of cylindrical bar, at $H = 0$.

5. Conclusions

The MRE obtained in the shape of a cylindrical bar by polymerization in longitudinal magnetic field has a matrix filled with Fe particle chains, parallel among themselves.

In longitudinal magnetic field, with $H \leq 200$ kA/m, the MRE shows no deformations of shape or volume, at torque $\Gamma = 0$. However, for fixed values of Γ , the turning angle of a MRE in the shape of cylindrical bar decreases with the increase of H .

By using the dipolar approximation and the model of linear elasticity, a new theoretical model which shows qualitatively, the mechanisms involved in the rotation of a cylindrical bar of anisotropic MRE subjected to the influence of a magnetic field, have been developed. The correction factors n and Ω in Eq. (8) lead to a reasonably good agreement between the theoretical values and the experimental data.

The obtained results can be used for the fabrication of rotary transducers or for manufacturing devices, which can perform rotation movements controlled by the variation of an external magnetic field.

Acknowledgements

The authors thank Dr. Erhardt Papp and Dr. Constantin Cheveresan (West University of Timisoara) for discussions relating to this paper. Also, the author conveys thanks to Dr. Marian Lita ("Polytechnica" University Timisoara) for X-ray micrographs and to Dr. Aurel Ercuta (West University of Timisoara) for magnetization measurements.

The WUT-JINR scientific projects and the grants of Romanian Governmental Plenipotentiary to JINR are acknowledged.

References

- [1] G. Filipcsei, I. Csetneki, A. Szilagyï, M. Zrinyi, *Adv. Polym. Sci. (Book series, Springer-Verlag)* **206**, 137 (2007).
- [2] L. Lanotte, G. Ausanio, C. Hison, V. Ianotti, C. Luponio, C. Luponio, Jr., *J. Optoelectron. Adv. Mater.* **6**(2), 523 (2004).
- [3] S. Abramchuk, E. Kramarenko, G. Stepanov, L. V. Nikitin, G. Filipcsei, A. R. Khokhlov, M. Zrinyi, *Polym. Adv. Technol.* **18**(11), 883 (2007).
- [4] H. J. Choi, and M. S. Jhon, *Soft Mater.* **5**, 156 (2009).
- [5] I. Bica, and H. J. Choi, *Int. J. Mod. Phys. B* **22**, 5041 (2008).
- [6] I. Bica, *J. Ind. Eng. Chem.* **15**, 233 (2009).
- [7] X. Zhang, S. Peng, W. Wen, and W. Li, *Smart Mater. Struct.* **17**, 045001-045005 (2008).
- [8] W. Hu, N.M. Werely, *Smart Mater. Struct.* **17**, 04502 (2008).
- [9] I. Bica, *J. Ind. Eng. Chem.* **15**, 605 (2009).
- [10] I. Bica, *J. Ind. Eng. Chem.* **15**, 759 (2009).
- [11] I. Bica, *J. Ind. Eng. Chem.* **15**, 773 (2009).
- [12] I. Bica, *Mat. Letter.* **63**, 2230 (2009).
- [13] I. Bica, *Mater. Sci. Eng. B* **98**, 89 (2003).
- [14] (a) I. Bica, *Mat. Sci. Eng. B* **166**, 94 (2010);
(b) I. Bica, *J. Ind. Eng. Chem.* **18**, 483 (2012);
(c) I. Bica, M. Balasoïu, A.I. Kuklin, *Solid State Phenomena* **190**, 645-648 (2012).
- [15] D. L. Huber, J. E. Martin, R. A. Anderson, D. N. Read, B. L. Frankamp, *Sandia Report Sand 8031* (2005).
- [16] X. Guan, X. Dong, and J. On, *J. Magn. Magn. Mater.* **320**, 158-167 (2008).
- [17] D. Yu. Borin, G. V. Stepanov, *J. Optoelectron. Adv. Mater.* **15**(3-4), 249 (2013).
- [18] I. Bica, E.M. Anitas, M. Bunoiu, B. Vatzulik, I. Juganaru, *J. Ind. Eng. Chem.* **20**, 3994-3999 (2014).
- [19] I. Bica, E.M. Anitas, L. Chirigiu, M. Bunoiu, I. Juganaru, R.F. Tatu, *J. Ind. Eng. Chem.* **22**, 53 (2015).
- [20] W. Hu, N. M. Werely, *Smart Mater. Struct.* **17**, 045011 (2008).
- [21] A. Ercuta, *J. Phys.: Condens. Matter* **20**, 325227 (2008).
- [22] O. Nguyen, Y. Han, S. Choi, N. M. Werely, *Smart Mater. Struct.* **16**, 2242-2254 (2007).
- [23] D. York, X. Wang, and F. J. Gordaninejad, *Intell. Mater. Syst. Struct.* **18**, 1221-1232 (2007).
- [24] G. V. Stepanov, D. Yu Borin, Yu L. Raikher, P. V. Melenev, N. S. Perov, *J. Phys.: Condens. Matter.* **20**, 204121-204130 (2008).
- [25] M. Balasoïu, I. Bica, Yu. L. Raikher, E. B. Dokukin, L. Almasy, B. Vatzulik, A. I. Kuklin, *Optoelectron. Adv. Mater. – Rapid Commun.* **5**(5), 514 (2011).
- [26] (a) M. Balasoïu, V.T. Lebedev, D.N. Orlova, I. Bica, *Crystallography Reports*, **56**(7), 1177 (2011);
(b) M. Balasoïu, V.T. Lebedev, D.N. Orlova, I. Bica, Y.L. Raikher, *J. Physics: Conf. Series* **351**, 012014 (2012).
- [27] D. Gunther, D. Y. Borin, S. Gunther, S. Odenbach, *Smart Mater. Struct.* **21**(1), 015005 (2012).
- [28] G.E. Iacobescu, M. Balasoïu, I. Bica (2013), *J. Supercond. Novel Mag.* **26**, 785-792 (2013).
- [29] E. M. Anitas, I. Bica, R. V. Erhan, M. Bunoiu, A. I. Kuklin, *Romanian Journal of Physics* **60**(5-6), 653 (2015).
- [30] O.V. Stolbov, Yu.L. Raikher, M. Balasoïu, *Soft Matter* **7**, 8484 (2011).
- [31] A.M. Biller, O.V. Stolbov, Yu.L. Raikher, *J. Optoelectron. Adv. Mater.* **17**(7-8), 1106 (2015).
- [32] M. Kallio, *The elastic and damping properties of magnetorheological elastomers*, VIT Publications 565, PhD Thesis, Tampere University of Technology (2005).
- [33] I. Mihalca, A. Ercuta, and C. Ionascu, *Sensors and Actuators A* **106**, 61 (2003).
- [34] I. Bica, "Physics of Solid Deformation", (in Romanian) University of Timisoara Press (1992).

*Corresponding author: balas@jinr.ru